Proceedings of the 17th International Conference on Nuclear Engineering
ICONE17
July 12-16, 2009, Brussels, Belgium

ICONE17-75588

A CASE HISTORY OF CFD SUPPORT TO ACCELERATOR DRIVEN SYSTEM PLANT DESIGN

Vincent Moreau[1]
CRS4
Pula, Sardinia, Italy

Luigi Mansani
Ansaldo Nucleare
Genoa, Italy

Maurizio Petrazzini
Ansaldo Nucleare
Genoa, Italy

ABSTRACT

The Integrated Project EUROTRANS, funded by the European Commission in the VI European framework program, was aimed at providing the advanced design of a multi purpose research oriented Accelerator Driven System (ADS), called eXperimenTal-ADS (XT-ADS), and the preliminary design of an industrial scale ADS, called European Facility for Industrial Transmutation (EFIT). One contribution of CRS4 (Centro di Ricerca, Sviluppo e Studi Superiori in Sardegna) has been to provide support to the overall plant design by means of Computational Fluid Dynamics (CFD) simulations. The simulations were required by the designer either for basic checking or in case of doubts on the validity of some technical options. We present four series of simulations which lead to the detection of unsatisfactory plant behaviour, related design modification and eventually control of the variant behaviour correctness. The first three simulation series deal with the EFIT design while the forth one deals with the XT-ADS design. In the first case, the simulation put in evidence a large recirculation zone under the reactive core that had to be removed for oxygen control concern. The recirculation zone is suppressed by modifying the shape of the core support grid. In the second case, we put in evidence a recirculation zone at the entrance of the pumping system above the core. This recirculation zone can lower the pump efficiency. The entrance shape was modified to eliminate the recirculation zone. In the third case, we check the behaviour of the passive Decay Heat Removal (DHR) heat exchanger. We show that while the primary coolant flow is globally organized as expected, some flow mixing limits the efficiency of the system. The system efficiency is restored by increasing its passive pumping strength. This is performed simply extending the Heat Exchanger shroud a half-meter in the bottom direction. In the last case, we investigate the capability of an external DHR system to withstand a long complete plant shutdown. The simulation encompasses about 6 hours of physical time, enough to understand the critical trends and infers that the DHR system may be not sufficient for its purpose. This result has suggested some modification to the design (i.e. surface treatment to improve metal wall emissivity) as well as to the accident management (i.e. restart primary pumps to eliminate fluid stratification). All these design improvements have been obtained in a reasonable amount of time thanks to the continuous collaboration and exchange of information between the CFD engineer and the designer.

NOMENCLATURE

ACS Above Core Structure
ADS Accelerator Driven System
CFD Computational Fluid Dynamics
CRS4 Centro di Ricerca, Sviluppo e Studi Superiori in Sardegna
DHR Decay Heat Removal
EFIT European Facility for Industrial Transmutation
EUROTRANS EUROpean research programme for the TRANSmutation of high level nuclear waste in an accelerator driven system

[1] Corresponding author: e-mail moreau@crs4.it

HX Heat eXchanger
LBE Lead Bismuth Eutectic
SGU Steam Generator Unit
RVACS Reactor Vessel Air Cooling System
XT-ADS eXperimenTal-ADS

INTRODUCTION

The Integrated Project EUROTRANS, funded by the European Commission in the VI European framework program, was aimed at providing the advanced design of a multi purpose research oriented ADS, called XT-ADS [1**]**, and the preliminary design of an industrial scale ADS, called EFIT [2**]**. An ADS consists in a sub-critical nuclear fission reactor coupled with a proton accelerator by means of a target system. A sub-critical system does not rely on delayed neutrons for the control of power change, but is only driven by a Spallation neutron source, thus control rods and reactivity feedback have very little or no importance. For more information on ADS and EUROTRANS see **[3]**, for a description of a target system see **[4]**.

In EUROTRANS, a large part is dedicated to numerical simulations, be it for thermal-hydraulics, neutronics, chemical control, structural control and so on. With the CFD applications that will be described hereafter, we would like to show that CFD simulation can, in some situation, be used for large scale design support. Moreover, it can provide critical information that was not currently available. This new possibility is related to the increase in commonly available computational power but also in the fast and continuous progress demonstrated by the commercial CFD software. These commercial CFD codes regularly include new tools allowing simplifications of the overall simulation process and the access to problems of increased complexity, at parity of manpower. All the simulations presented here have been performed with Star-CD (from CD-Adapco **[5]**) suite of software. Geometries have been built with Star-Design, meshing has been done with a combination of Star-Design, Proam and Starccm+, and simulations have been performed with Star-CD (version 4.02) for the EFIT simulations and Starccm+ (version 3.02) for the XT-ADS simulation. The default setting for turbulent flows has been used: standard k-ε for Star-CD and realizable k-ε for starccm+, together with standard wall functions.

We are well aware that the predicted results may not be quite accurate. Errors are introduced at each step of the numerical setting: approximation of the geometry, of the physics and of the model averaged equations. We have also discretization errors, both spatial and temporal. No attempt has been done to quantify these errors. In particular, no estimate has been done on potential numerical diffusion caused by tetrahedral cells.

Another key point required to treat large scale design features is the oversimplification of large parts, possibly complex, of which we know the global behaviour. Only this global behaviour has to be correctly reproduced (it may come from constructor specifications or, alternatively, the part has not been yet designed in detail). A typical example is the heat exchanger. In principle, a HX could be quite accurately simulated with a CFD tool, taking into account all details like the hundreds of tube, the support grids, etc. This would require millions of cells and large man/computer resources without giving useful insight for the global design. Instead we make use of the porous media, of their distributed resistance factors and also of the localized (baffle) hydraulic resistance. The heat exchange is mimicked by a distributed enthalpy source term with a simple law depending on the local temperature, a critical time, and sometimes the local flow velocity. The coefficients are adapted to conform to the expected (or prescribed) global behaviour. This technique has been extensively used for heat exchangers, nuclear core, pump and by-pass flows.

The simplification procedure, while absolutely necessary, is extremely case and purpose dependent. Therefore, the CFD engineer should carefully review these simplifications together with the designer to clearly understand and control their consequences.

The added value of CFD comes from its ability to portray results with visualization tools. And considerations are often based on basic observation of the predicted flow velocity or temperature fields. That is why this paper consists mainly in a collection of images. Most of these images are good quality and should be looked at with a 200% zoom on a computer to be correctly appreciated. The understanding of the geometry and the predicted flow requires usually much more that what is shown here. Much more detail on the computational geometry, the mesh, and the flow characteristics, including animations of transient flows, can be found at the main author home page **[6]**.

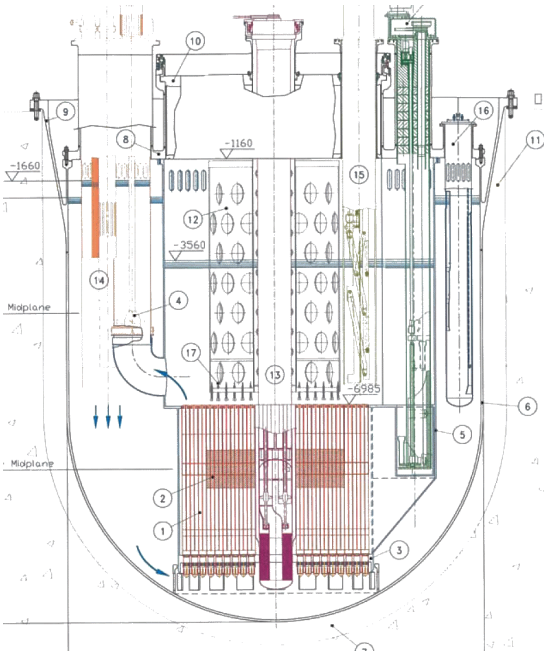

Figure 1: initial EFIT design

Support to the EFIT design

EFIT is designed as a waste burner machine (it is fueled by Minor Actinide waste - Uranium –free fuel) and as an electricity production plant **[2]**. It is shown on Figure 1. The foreseen primary coolant is pure lead, whose physical properties have been recently carefully reviewed and gathered in **[7]**. From the thermo-dynamical point of view, EFIT is an approximately axial-symmetrical loop, the lead being heated in the central core while rising, and being cooled down in SGUs while flowing down laterally. It is driven by pumps in rising pipes.

First of all, an axial-symmetrical approximated simulation has been performed to build confidence with the physics involved and the main characteristics of the flow. It allows also to understand which were the region for potential further and deeper investigation. The flow velocity and the fluid temperature (with reference to 400 ^{o}C) are shown on Figure 2.

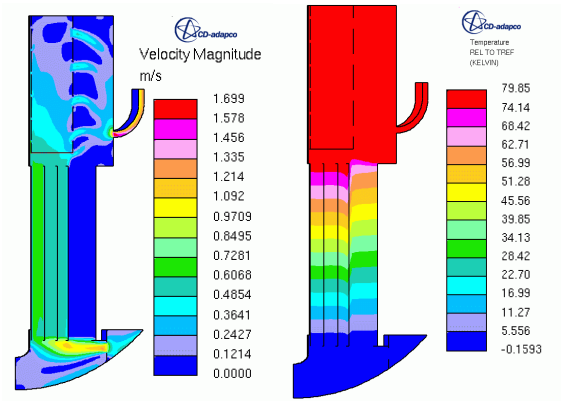

Figure 2: 2D simulation of the EFIT design, colored on the LHS by the velocity magnitude and on the RHS by the temperature.

The simple observation of these pictures identified one obvious defect and another potential one.

The obvious defect is that the flow enters the under core region almost horizontally with the bottom-most part almost stagnant consisting in a large slowly re-circulating zone. This is not acceptable because of corrosion and sedimentation matters. In effect, all the lead must be subject to regular purification and control of oxygen concentration. A slowly re-circulating zone could trap fluid (or solid) particles for a large time.

The potential trouble lies in the flow acceleration at the entrance of the pipe leading to the driving pump. While the 2D approximation is extremely rough, one could expect both an excessive velocity (bounded to 2m/s for corrosion concern by functional requirement) at the duct entrance and a recirculation in outlet of the bending duct potentially damageable to the pump performance.

A third consideration could be also confirmed by this simulation. It is that the flow rates in the different parts of the core are completely controlled by the hydraulic resistance in the core and absolutely not by the way the fluid is fed to the bottom region. Similarly, the average temperature in outlet of the different core region depends only of the mass flow rates (for a given energy deposition) and can be made strongly homogeneous. This consideration is important for the CFD point of view because it justifies the choice of simulating separately the bottom and the top regions in 3-dimensional configuration.

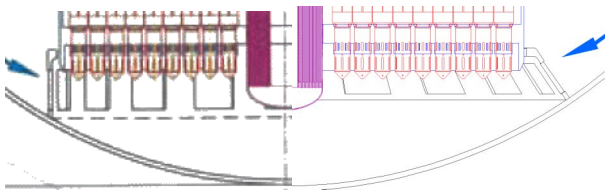

Figure 3: EFIT bottom grid before (left) and after (right) modification

The bottom re-circulating zone

To remove the bottom large re-circulating zone, the designer decided to modify the shape of the bottom grid, making it locally orthogonal to the reactor vessel. The configuration before and after modification is illustrated in Figure 3.

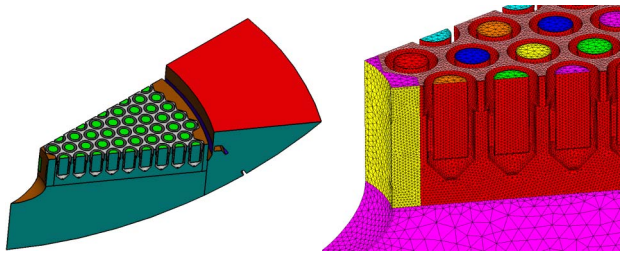

Figure 4: Computational geometry in updated bottom grid configuration (left) and related mesh detail (right).

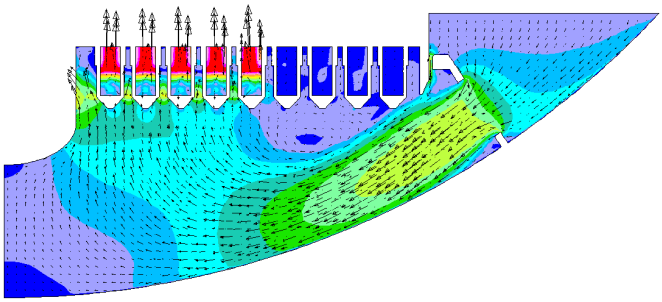

Figure 5: velocity field for the updated bottom grid configuration.

The updated bottom grid configuration has been tested with a full 3D CFD simulation (in fact 30 degrees, taking into account the symmetries). The computational domain is shown on Figure 4 together with a mesh detail. The velocity field on one vertical

plane section is shown on Figure 5. The recirculation zone at the bottom has been removed, validating the design variant.

Above core 3D simulations

Recognizing a potential trouble for the driving pump, the design has been slightly modified. The tentative design of the region near the pump connector is shown on Figure 6. Obviously, the information given by the 2D simulation was not sufficient to get a clear picture of the situation. Therefore a 3D simulation has been performed. The symmetries allowed to reduce the computational domain only to a 90 degrees angular sector.

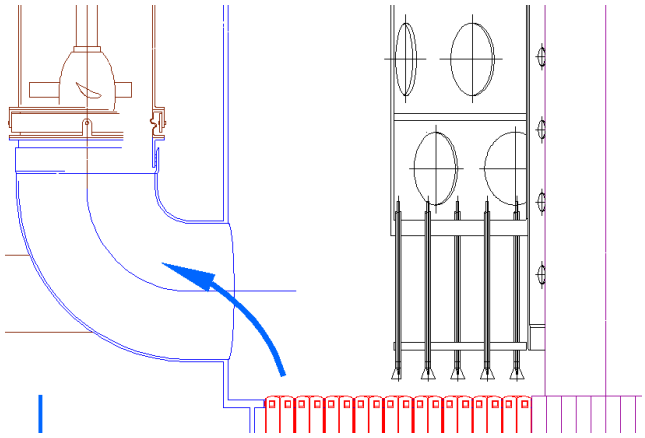

Figure 6: tentative design of the above core part

The computational geometry is rather complex. In Figure 7, we show the solid internal parts that had to be removed from the fluid envelop together with a part of the mesh. This solid part represents the Above Core Structure (ACS) whose design is far from being yet fixed. While the simulated flow is rather complex, with large scale three-dimensional structure, the only critical point was to control the flow entering the pump duct. This is done by observing the velocity field in the vertical plane supported by the core and the pump axis and shown on Figure 8. In this simulation, the horizontal plate shown in Figure 7 was treated as a slightly resisting porous media. Apart from an excessive velocity at the inner side of the bending connector (red is indicating a speed over 2m/s), the main problem is the recirculation and strong lateral velocity gradient in the riser where the pump should be located. Such a flow could dramatically lower the pump efficiency.

Two simulations were performed (not shown here), making the flow freely enter from above in the ACS or being completely blocked. That is, the horizontal plate shown in Figure 7 was considered respectively as a fluid or a solid region. No noticeable differences were found for the velocity profile inside the duct. As the simulations were requiring a large computing resource, the mesh being about 4.25 million tetrahedral cells, and because we had to test numerous variant of the geometry, we decided to build a simplified 3D parametric model.

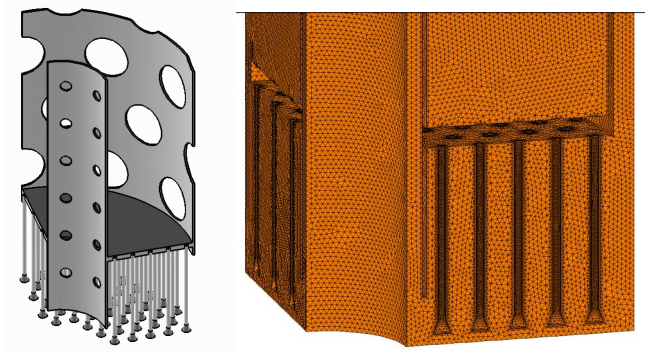

Figure 7: Above core full 3D simulation. Left, solid and porous internal parts. Right, mesh detail.

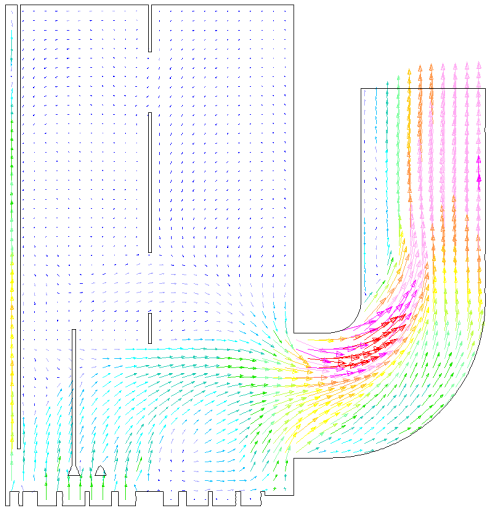

Figure 8: above core full 3D simulation. Velocity field on the plane supported by the core and the pump axis.

Above core simplified parametric model

The simplified parametric model gets rid of all the small scale features not strictly necessary considering the objective which is to suppress the recirculation and lower the lateral velocity gradient in the duct upper part. That is, all the fuel assemblies outlets have been gathered into one unique inlet, the ACS sensors (the vertical tubes in Figure 6) have been removed and the ACS is now a structure completely blocking the flow. The tetrahedral mesh is reduced in this way to about 600k cells. The mesh density has been chosen in such a way that the recirculation zone can be clearly identified and the effect of the geometrical changes clearly understood. Moreover, the outlet boundary interacts in a non physical way with the extension of the recirculation zone and only qualitative information can be obtained.

The parameterization concerned the height of the ACS horizontal plate and the height at which the pump pipe connects

the main reservoir. The simulations went much faster due to the simplified geometry and some velocity fields can be appreciated on Figure 9. As it can be seen, none of them gives a satisfying result in the duct. By the way, a small improvement is obtained lowering the plate clearly below the level of the top of the connector (Figure 9, case d). This information has to be kept in mind when the details of the above core structure will be better defined.

An alternative approach had to be found out to better control the duct flow. A standard procedure to regularize a flow is to put it in a convergent channel. Here, the problem is complicated by the fact that there is not a lot of place at disposal. So, we have been obliged to install the convergent channel in the bended part of the duct. The riser diameter being imposed by the pump size, the convergent channel had to be realized by enlarging the connector entrance. After a few tests, we arrived to a connector initially rectangular progressively turning circular while bending upward. The induced contraction was ¾ from 0.8 to 0.6m^2. The geometry and corresponding flow field are shown on Figure 10. The rising flow is now much more regular and in any case regular enough for a correct functioning of the pump.

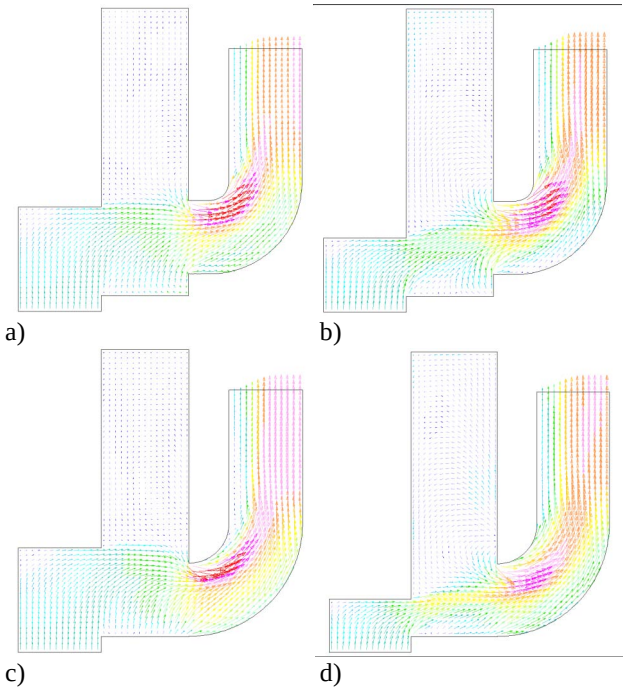

Figure 9: above core parametric simulations. Velocity field for different geometries: a) high ACS, high connector, b) medium ACS, high connector, c)high ACS, low connector, d) low ACS, low connector.

A residual problem in the above configuration is an excessive flow maximum velocity, above 3m/s, while the limit should be 2m/s. The region of excessive velocity is extremely localized at the top of the duct entrance. The problem can be alleviated by smoothing this region. As the containment lateral wall should not be altered, the smoothing is better performed by adding a solid "smoother" in the inside. This idea is illustrated on Figure 11, showing the geometry variant and the flow field. The effect of the "smoother" is to lower the maximum velocity by about 1m/s and to additionally regularize the rising flow. This feature is independent of the gain obtained by lowering the ACS plate, so the maximum velocity limit of 2m/s should be attainable.

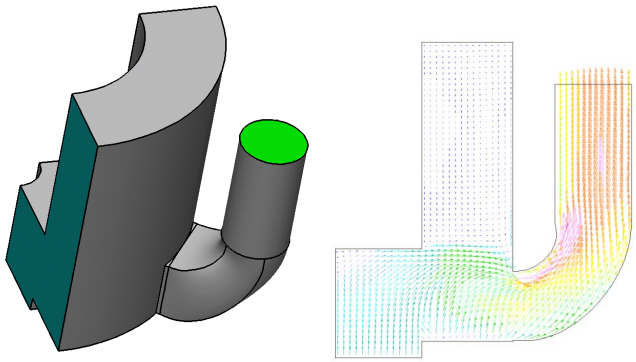

Figure 10: above core simplified geometry with a converging connector. Geometry on the left, velocity field on the right.

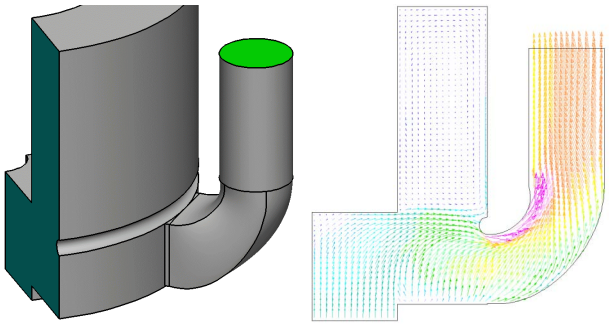

Figure 11: above core simplified geometry with a converging connector and a "smoother". Geometry on the left, velocity field on the right.

The geometrical variants issued from the CFD simulations are not neutral from the structural and ease of manufacture point of view. Moreover, the velocity limit could be bypassed by using special surface treatments in small critical regions. Therefore, only the basic idea of making an enlargement of the connector entrance has been yet incorporated in the design.

EFIT down-comer under DHR condition

The next simulation concerns the down-comer part of the EFIT vessel. It consists of the riser above the pump propeller, the connector between the pump and the steam generator unit (SGU), the DHR Dip Cooler and the plenum between the Inner

and the Reactor vessels down to the bottom support grid. A top view of the part under exam can be seen in Figure 12, together with the computational geometry.

The final objective of the simulations was to control that the flow would let the Dip Cooler work as expected under DHR condition.

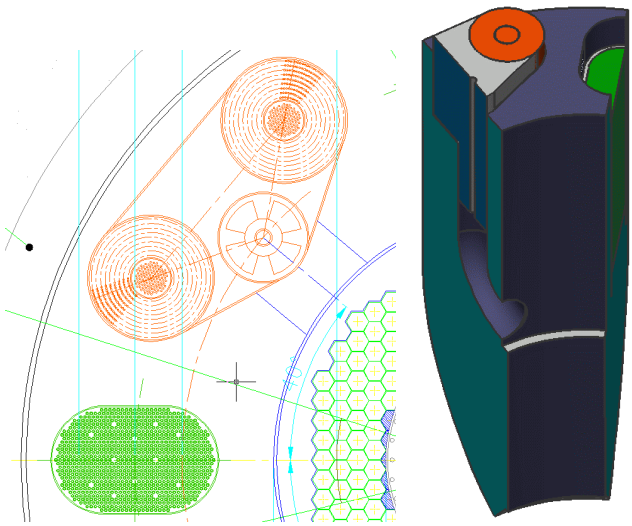

Figure 12: down-comer simulation. Left, horizontal section of the geometry. Right, computational geometry: in orange the SGU, in green the DHR cooler.

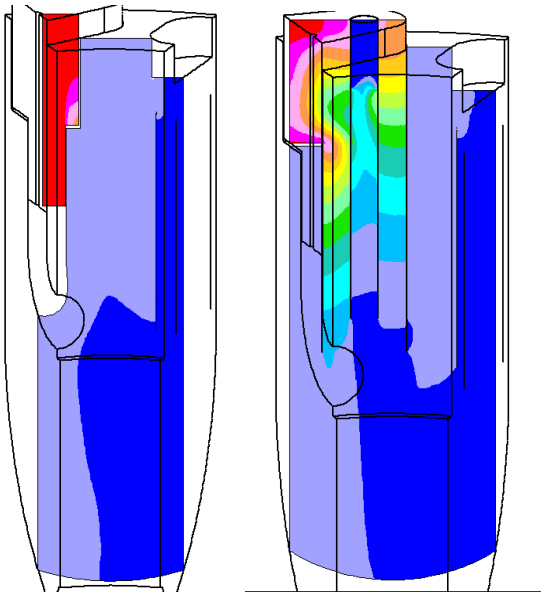

Figure 13: down-comer simulation, temperature field under nominal condition. Temperature range: 400-480 ^{o}C.

As before, the first step has been to make a stationary simulation of the entire part under nominal condition. The geometry can be made sufficiently simple to be treated directly in 3D. This can be done treating the heat exchangers as porous media.

The simulation under nominal condition confirmed the expected behavior of the flow. Under nominal condition, the Dip cooler works very little, but enough to keep the down-comer plenum relatively cold, thus compensating for the eventual heat flux through the walls. The geometry is quite intricate and it is relatively difficult to get a global view of the system from only a few pictures. Nevertheless, we show the temperature field on two tangential planes passing through the Riser and the SGU axis on Figure 13. Then, we have performed the simulation under DHR condition, simply deactivating the heat exchange in the SGU, lowering the inlet temperature from 480 to 440 ^{o}C and reducing the mass flow rate to about 12% of the nominal value.

The relative importance of buoyancy to inertia can be measured by the ratio of Grashof to Reynolds number Gr/Re^2. Due to the combined effect of a small velocity (about 5 cm/s) at the SGU outlet and a relatively large buoyancy (about 50 kg/m^3 of density variation), this number is of order 100 under DHR condition, and the fluid rises up as soon as leaving the SGU outlet to enter the Dip Cooler. Unfortunately, as can be seen on the temperature field, shown on Figure 14, some mixing appears between the hot flow leaving the SGU and the cold flow leaving the Dip Cooler. The result is that the flow entering the Dip Cooler is colder than expected and the Dip Cooler performance is lowered.

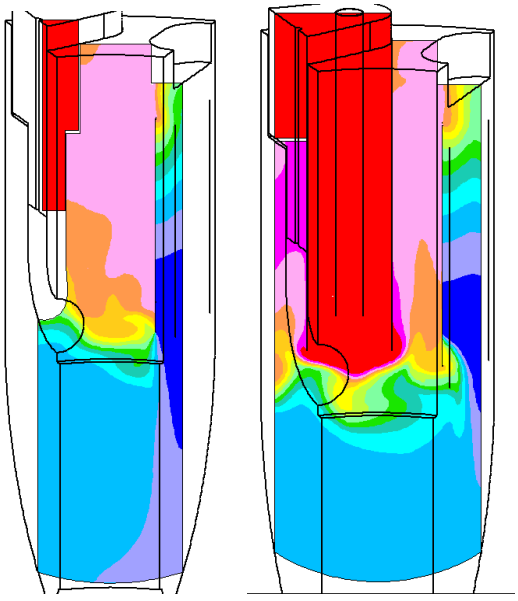

Figure 14: down-comer simulation under DHR condition with the original geometry. Temperature range: 400-440 ^{o}C

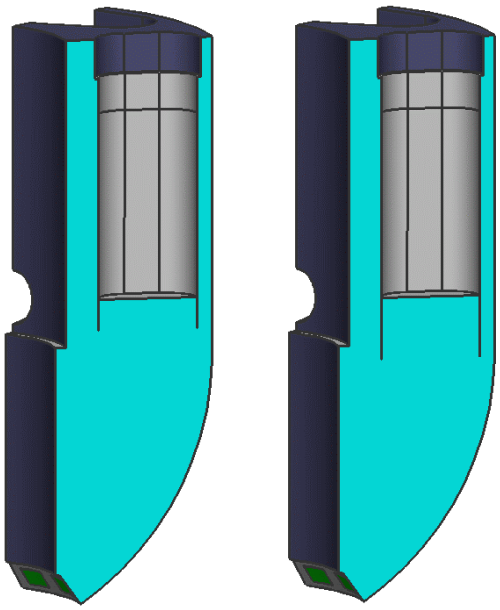

Figure 15: down-comer geometry. Left, the original one. Right the modified geometry with the elongated shroud.

Once put in evidence, and due to the availability of space, this problem can easily be solved by extending the Dip Cooler shroud somewhat downward. The effect is two-fold, first, it limits the bottom mixing and second, it increases the Dip Cooler pumping power. Simulations showed that an extension of only half meter would be sufficient to reach the desired goal. The difference in geometry is shown on Figure 15 and the temperature field with the updated geometry is shown on Figure 16.

The simulation with the updated geometry gave a globally satisfying result. By the way, it was performed as a stationary simulation and the convergence was not excellent (even if the flow field did not show variations). Thus, to get more confident with the solution, we decided to pursue the simulation in transient mode. In this way, we could check whether the stationary solution was stable in the transient framework.

The switch to the transient framework was not such an easy task. Small defects of the mesh which were formerly without consequence now made the solution diverge. Moreover, the cell number (about 1 million), quite reasonable for a stationary simulation, became large for a transient one. From the observation of the stationary solution, we could see that it was useless to simulate the flow from the rising pipe up to the bottom of the SGU. By taking off this part, the cell number could be made 60% smaller (and the main mesh defects also eliminated).

The ultimate modification we had to perform was to extend the two outlets numerically. This prevents the flow to present locally some inlet flow in outlet, which in stationary simulation leads to no real consequence (only a warning saying that counter measures are taken), but in transient simulation leads to the crash of the simulation.

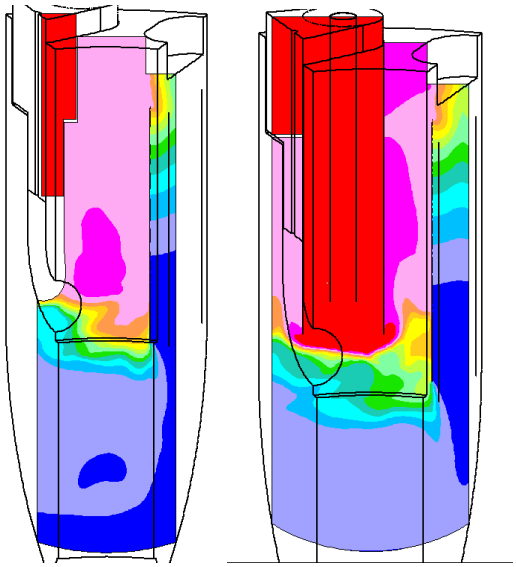

Figure 16: down-comer simulation under DHR condition with the modified geometry.

With these modifications, the simulation could easily be performed in the transient framework, after having been converged in the stationary framework.

The time scale involved in the simulation is about one minute. We made the flow field evolve for three time scale to get a clear picture of the asymptotic solution. The time of simulation was relatively long, giving about 15s of physical time by computing day on a PC with 4 CPUs AMD Opteron 2.2 GHz and 16 GByte RAM.

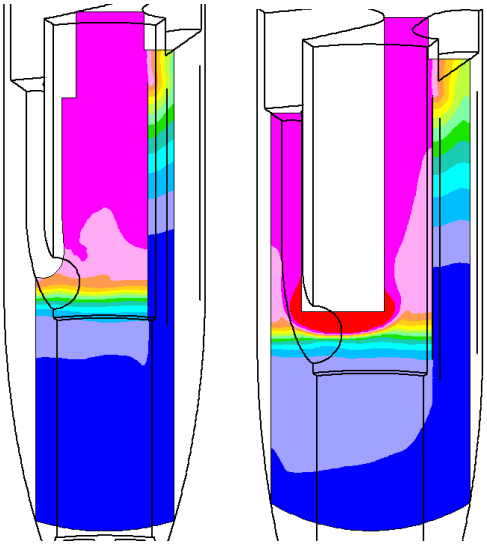

Figure 17: down-comer transient simulation under DHR condition with the updated geometry after 180s.

The time evolution showed a slow strengthening of the thermal stratification and a consequent further diminution of the mixing at the SGU outlet. At the end of the transient simulation, the performance of the Dip Cooler had increased by about 5-10%. The corresponding temperature field can be seen on Figure 17.

Support to the XT-ADS design

Two systems are provided in the XT-ADS [5] for the DHR function to increase diversity and redundancy, i.e.

- The safety grade part of the Secondary and the Tertiary Cooling system, (normally used also for the full power removal): DHR System number 1;
- The safety-grade Reactor Vessel Air Cooling System (RVACS): DHR system number 2 (it is called upon in case of unavailability of the Secondary System).

The last simulation presented here deals with the XT-ADS design and had the goal to understand whether the RVACS (DHR number 2) is able to maintain the vessel temperature below the limit in case of station blackout with concomitant unavailability of the DHR system number 1. The foreseen XT-ADS primary coolant is LBE whose physical properties can be found in [7]. While built for more general purpose (ADS prototype and irradiation machine), the XT-ADS is from the CFD point of view very similar to the EFIT.

The computational geometry under exam was built from the Ansaldo design shown on Figure 18.

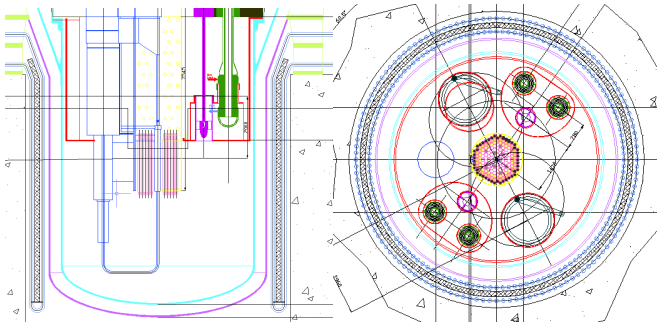

Figure 18: Ansaldo design of the XT-ADS

Accepting some liberty with the original design, we considered that we could simulate only half the domain from approximated symmetries. This approximation does not seem to have effects on the phenomena which are under exam but allow to halve the mesh number for the same accuracy. Inversely, a careful examination of the geometry lead us to incorporate very small details of the geometry when they were potentially leading to large effects on the flow. Mainly, we had to take into account several by-pass flows, even if a rather crude way. The resulting geometry has therefore a mix of large simplification, the core and the heat exchangers being treated as porous materials, and crucial small details (the by-passes). It is illustrated on Figure 19.

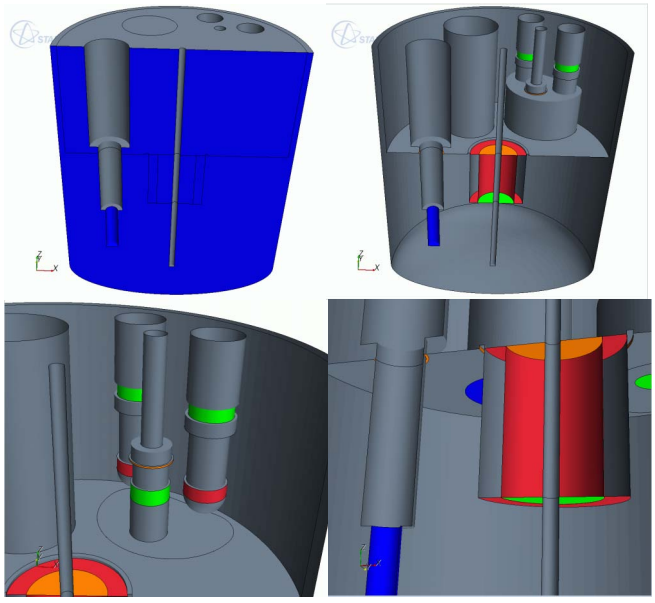

Figure 19: Computational geometry of the XT-ADS

Simulation under stationary nominal condition

The simulation under stationary nominal condition was relatively complex to setup. The problem was to obtain the correct expected value of the flow rates across all critical sections as well as the expected pressure drops. Many of these were in fact specified.

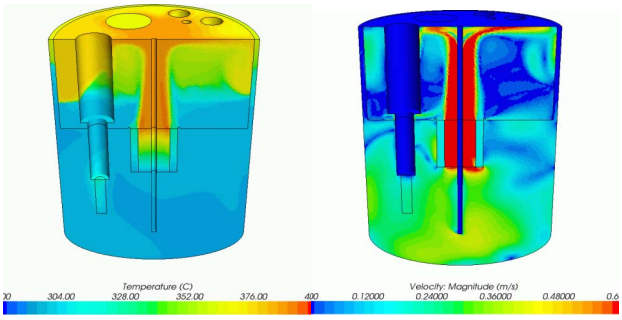

Figure 20: temperature and velocity flow on the symmetry axis for the XT-ADS nominal condition.

We used a trial and error method, adjusting the distributed pressure loss coefficients in the porous regions and the localized pressure loss coefficients through the by-pass interfaces. As the flow reacted fast and well to the manipulation of the coefficients, it has been possible to obtain the desired configuration of the flow within a few hours. Moreover, the process has been fastened by using a coarse mesh of 300k cells at the beginning of the procedure for the preliminary settings and increasing this number when arriving to the fine tuning. The final mesh is composed of 1.7 millions polyhedral cells.

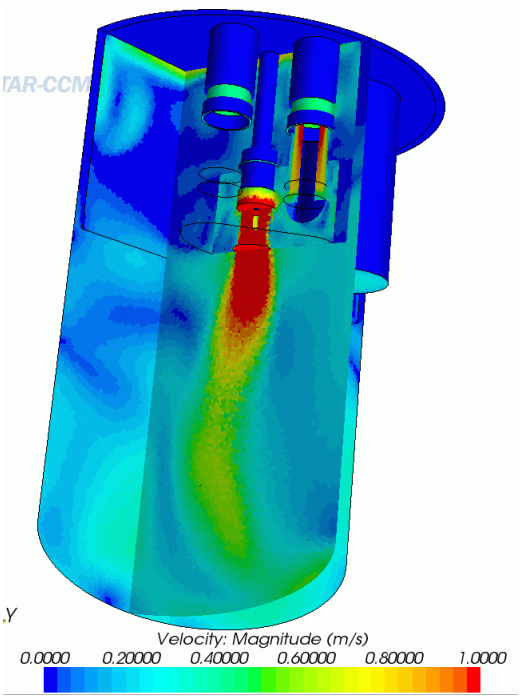

Figure 21: XT-ADS nominal condition, velocity field focused on the fluid flowing out of the pump.

The flow temperature and velocity field on the symmetry axis under nominal condition is show on Figure 21. The flow velocity field below the pump is shown on Figure 21. This figure shows that, as expected, there is no dead zone in the bottom region, the jet flow from the pump outlet being strong enough to eliminate it.

The only unexpected feature found out from the stationary solution under nominal condition is the large amount of cold fluid in the confined region above the core. This cold flow comes from the by-pass flow at the periphery of the core and of the target loop at the main plate level. These by-pass flows are quite low compared to the flow from the core but they fill the bottom part of the hot plenum while the core flow fills the upper part of the hot plenum and the result comes from the strong buoyancy effect limiting the mixing between the hot and cold flows. This unexpected feature is considered as positive because it gives an improved heat capacity storage against eventual plant over heating.

Simulation under Emergency DHR condition

The Emergency DHR incidental operating conditions are based on an unlikely postulated black out (in which all sources of energy simultaneously disappear) with concomitant unavailability of the secondary system (only the DHR system 2 is available):

- Loss of the beam: linear decay in 1s
- Loss of the pumps: linear decay in 3s
- Loss of the HX cooling: linear decay in 3s
- Loss of the target HX heating: linear decay in 3s.

The initial condition is obtained from the nominal stationary condition run in transient mode for some time. After one second, the heat source reverts to a decay heat source which is 7.2% of the original source but concentrated only in the active part of the core. The decay heat then decreases according to a curve elaborated in Ansaldo Nucleare, reaching 1.3% after 20,000s.The decay heat needs to be eventually compensated by some heat loss to avoid overheating if the incidental condition persists for a long time. For this purpose, a completely passive RVACS system has been designed allowing to loose heat across the lateral external wall through thermal radiation. This system has also been designed such has to avoid a local freezing of the Lead. Its efficiency scales approximately with the third power of the local wall temperature. It is therefore quite dependent on the flow thermal stratification close to the external wall.

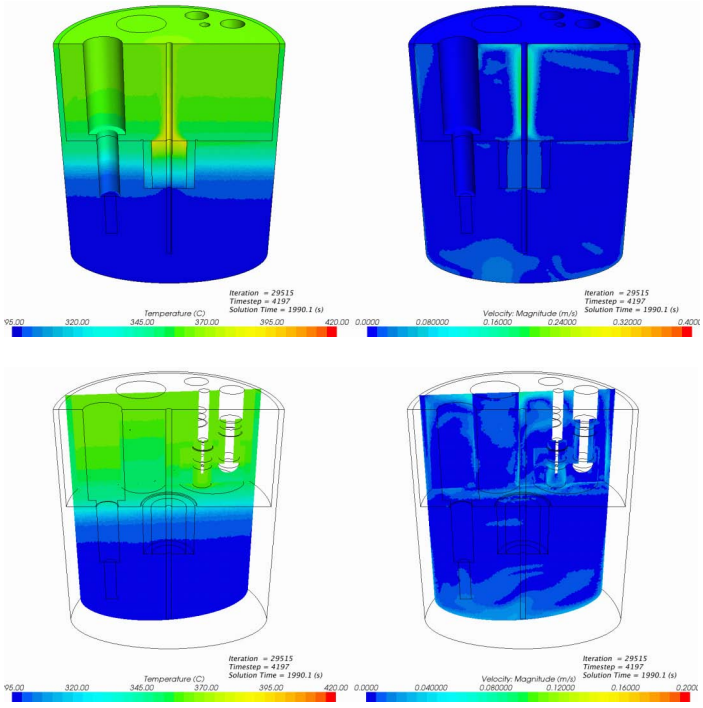

Figure 22: DHR transient simulation after 2,000s. Temperature on the left, velocity on the right. Below, the view plane is crossing the pump axis.

The simulation encompasses 20,000s of physical time and required about 2 months of calculation on 20 CPUs (on a PC cluster of Dual CPU dual-core AMD opteron 2218, 2600Mhz, 16GB RAM DDR2 ECC). Nevertheless, the first days of simulation allowed to reach only about 2s of physical time per day. Fortunately, the maximum velocity, reached in the pump region, strongly decreased in time and we could multiply by a factor of 5 the initial time step after 10s of physical time simulation. This process continued during all the simulation and

the time step could be progressively increased from 0.02s to 2s. When the pump is working, there should be a level difference (about 0.9 m) between the inner and outer upper free surface. This level difference should almost disappear when the pump is out, inducing additional mass transfer. This aspect is not taken into account in the simulation but should have effects only on the short time behavior of the flow, therefore only medium and large time behavior of the transient simulation are considered as fully meaningful.

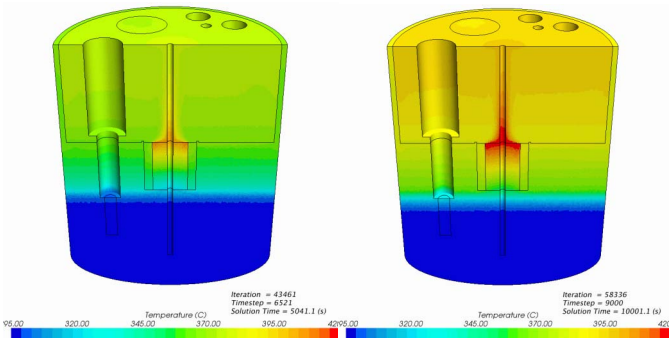

Figure 23: DHR transient simulation after 5,000s (left) and 10,000s (right). Temperature field.

After 2,000s, a large part of the initial kinetic energy of the flow has been consumed through turbulent dissipation and a new flow circulation is established, driven by the buoyancy induced by the core decay heat release and heat loss through the external wall. The temperature and flow velocity is shown on Figure 22.

Continuing the simulation, the flow continues to quiet down and the temperature slowly increases. The temperature on the symmetry axis is shown at time 5,000 and 10,000s on Figure 23. The temperature and flow velocity at the end of the simulation after 20,000s is shown on Figure 24.

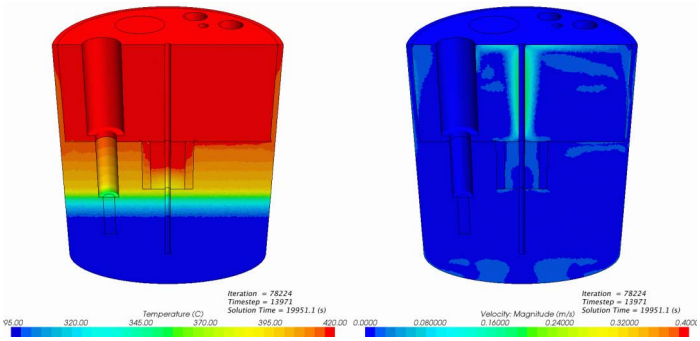

Figure 24: DHR transient simulation after 20,000s. Temperature on the left, velocity on the right.

.

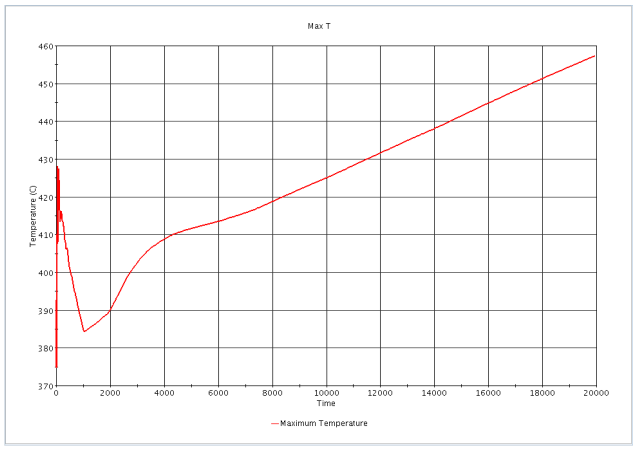

Figure 25: Time evolution of the maximum temperature during the DHR transient.

The evolution of the maximum temperature and of the heat flux to the RVACS are shown respectively on Figure 25 and Figure 26. Both curves exhibit a strong linear behavior for more than 10,000s. This is rather surprising because of the strongly non-linear underlying causes. Nevertheless, it allows to make simple extrapolations to evaluate the time at which the maximum reactor vessel temperature reaches the limit temperature (about 550°C), which is about 12 hours. As the Reactor Vessel wall temperature increases the contribution of irradiation to the total decay heat removal become more and more significant. As a consequence the evolution of the curve is not linear but its slope decreases. The time when the heat losses compensate exactly the decay heat is much longer, about 50 hours (this time is confirmed with simplified calculations with 1D specific code). At the end of the simulation, the heat loss is already about one third of the decay heat. It is worth noting that the minimum temperature remained extremely stable varying by less than 5K during all the transient

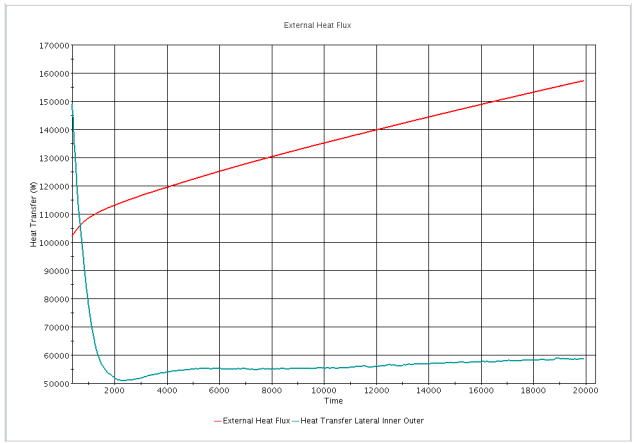

Figure 26: Time evolution (in red) of the heat flux to the RVACS during the DHR transient.

This result is considered encouraging but not totally satisfying. It is required that the reactor vessel temperature limit is never reached. This has required some modification to the design such as a surface treatment to improve the metal wall emissivity as well as to the accident management, imposing the restart of, at least, one primary pump within 12 hours from the accident to eliminate the fluid stratification. A grace time of 12 hours is deemed sufficient for the unlikely postulated event.

CONCLUSION

We have presented several CFD simulations in support to the EFIT and XT-ADS design performed in the framework of the EUROTRANS FP6 program. These simulations have been performed with the latest versions of the Star-CD suite of software allowing to confront with always more complex situations. They encompassed large parts of the reactors and were used both for checking the design features and to evaluate some variant when some defect was discovered. Basis for success was a careful examination of all the potentially important elements of the design and because we reverted to extremely simplified treatments of highly complex objects like the core or the HXs. This could not have been possible without the deep involvement of the designer both for the description of the problematic and for the analysis and control of the intermediary and final results.

ACKNOWLEDGMENTS

The authors appreciate the efforts and support of all the scientists and institutions involved in EUROTRANS and the presented work, as well as the financial support of the European Commission through the contract FI6W-CT-2004-516520.

REFERENCES

[1] D. De Bruyn, D. Maes, L. Mansani, B. Giraud, “From Myrrha to XT-ADS: The Design Evolution of an Experimental ADS System”, *Eighth International Topical Meeting on Nuclear Applications and Utilization of Accelerators (AccApp’07), Pocatello, Idhao, USA, July 30 – August 2, 2007*

[2] A. Barbensi, G. Corsini, L. Mansani, C. Artioli, G. Glinatsis, “EFIT: The European Facility for Industrial Transmutation of Minor Actinides”, *Eighth International Topical Meeting on Nuclear Applications and Utilization of Accelerators (AccApp’07), Pocatello, Idaao, USA, July 30 – August 2, 2007*

[3] J.U. Knebel, H. Aït Abderrahim, L. Cinotti, L. Mansani, F. Delage, C. Fazio, M. Giot, B. Giraud, E. Gonzalez.8, G. Granget.4, S. Monti.9, A.C. Mueller, "European Research Programme for the Transmutation of High Level Nuclear Waste in an Accelerator Driven System (EUROTRANS)", Proc. 9th Int. Exchange Meeting on Partitioning & Transmutation, Nimes France, September 25-29 2006.

[4] Bianchi, F., et al., Thermo-hydraulic analysis of the windowless target system, Nucl Eng Des (2008), doi: 10.1016/j.nucengdes.2007.10.026

[5] CD-Adapco web site (Accessed March, 20, 2009)
http://www.cd-adapco.com

[6]Vincent Moreau professional web site (Accessed March, 20, 2009)
http://people.crs4.it/moreau/HTML/EUROTRANS/index_EUROTRANS.html

[7] Handbook on Lead-bismuth Eutectic Alloy and Lead Properties, Materials Compatibility, Thermal-hydraulics and Technologies, Nuclear Energy Agency 2007 Edition **http://www.nea.fr/html/science/reports/2007/nea6195-handbook.html**